Limnol. Oceanogr., 40(2), 1995, 393–410

In situ methods for measuring the inherent optical properties of ocean waters

Annick Bricaud[1]
College of Oceanography, Oregon State University, Corvallis 97331, and Sea Tech Inc., POB 779, Corvallis 97339

Collin Roesler and J. Ronald V. Zaneveld
College of Oceanography, Oregon State University

Abstract

In situ attenuation (488 and 660 nm), absorption (488, 676, and 750 nm), backscattering (at 488 nm), and stimulated fluorescence were determined as functions of depth in oceanic and coastal waters off Oregon, using both commercial instruments and recently developed prototypes. The inability to perfectly constrain scattered light in these instruments necessitates correction to retrieve accurate optical coefficients. Because scattering is usually one order of magnitude higher than absorption, the correction is most critical for absorption coefficients. A correction procedure based on values obtained with the absorption meter in the infrared region (750 nm) was used to correct the measured spectral absorption coefficients. Realistic values of the backscattering coefficient were obtained from a prototype instrument, although accurate calibration could not be performed for this study.

These measurements resulted in the first-ever data set of in situ profiles of attenuation, absorption, scattering, backscattering, and the backscattering ratio. The blue and red attenuation coefficients were tightly correlated, with a relationship varying from site to site. The red-to-blue absorption ratio varied both from site to site and vertically, indicating changes in the relative concentrations of chlorophyllous (phytoplankton) and nonchlorophyllous (biogenous or mineral) particles. The backscattering ratio also appeared to be very sensitive to vertical changes in particle composition. The in situ scattering coefficients were compared to those estimated with a Mie scattering model, using measured particle size distributions and particulate absorption coefficients as input parameters. By allowing the real part of the refractive index of particles to vary over the range of realistic values, convergence between measured and modeled values was obtained.

Light penetration in the ocean is ruled by the scattering and absorption properties of the various substances. These two inherent optical properties are, therefore, with the attenuation coefficient (c, the sum of the scattering, b, and absorption, a, coefficients), the fundamental parameters in radiative transfer studies and in the interpretation of apparent optical properties. More specifically, the absorption and backscattering (b_b) coefficients directly determine the diffuse reflectance of the ocean and thus are integral to the interpretation of remote sensing data (*see* Gordon and Morel 1983). The absorption capacity of living phytoplankton, which now can be derived from total particulate absorption through various models (Morrow et al. 1989; Roesler et al. 1989; Bricaud and Stramski 1990), is also a critical input parameter for predicting the phytoplankton growth rate and modeling primary production (Kiefer and Mitchell 1983; Morel 1991).

According to their definition, the inherent optical properties are not easily measured because of instrumentation limitations on the separation of absorbed and scattered photons and thus are not currently determined in situ. The exception is the broadband transmissometer from which c is derived and commonly used as an index of seston concentration (e.g. Pak et al. 1980, 1984).

The most widely used method for determining a is spectrophotometric analysis of discrete water samples. Particulate absorption coefficients are commonly determined by the filter-pad technique (Trüper and Yentsch 1967). The values of a provided by this method are subject to uncertainty, especially at low optical densities, due to the optical properties of the filter pad which cause variations in the pathlength amplification inside the filter associated with filter type (Mitchell 1990) or phytoplankton species (Bricaud and Stramski 1990). Absorption by the dissolved fraction (operationally defined as whatever passes through the filter) is determined in cuvets. Depending on the optical configuration of the spectrophotometer (Bricaud et al. 1981), we may also need scattering corrections for accurately determining dissolved absorption coefficients.

We can measure a directly on individual particles by

[1] Present address: Laboratoire de Physique et Chimie Marines, Université Pierre et Marie Curie and CNRS, BP 8, 06230 Villefranche-sur-Mer, France.

Acknowledgments

This research was supported by Oregon State University through the Visitor Exchange Program P-1-0480 and by Sea Tech, Inc., through in-house funds (A. Bricaud), by NASA Graduate Student Researchers Program grant NGT-50681 (C. S. Roesler), and by ONR grant N00014-90-J-1132 (J. R. V. Zaneveld).

We thank Casey Moore for continuous assistance with the optical measurements during the cruise, Susanna Neuer for providing the chlorophyll concentrations, and Jim Kitchen, André Morel, and Scott Pegau for comments on earlier drafts of the manuscript.

microspectrophotometry (Iturriaga et al. 1988). Other recent techniques include the use of an integrating cavity (Fry and Kattawar 1988; Fry et al. 1992) or of an electro-optic radiance distribution camera system (Voss 1989). However, all these methods are time consuming, require (except for the last technique) water sampling, and provide only discrete values for absorption. Thus the need has persisted for a continuous, routine measurement of in situ absorption, even if it may be less discriminative with respect to the different absorbing components. Several techniques, all with inherent limitations, have been used with that aim for many years (*see* Zaneveld et al. 1990). Zaneveld et al. (1990), renewing the old concept of the reflective tube, developed absorption meters at different wavelengths as a first step toward developing a spectral absorption meter covering the whole visible range (Zaneveld et al. 1992; Moore et al. 1992).

Despite its crucial importance in reflectance modeling, very few measurements of the in situ b_b have been made. Most of the values introduced in models (e.g. Morel 1988; Gordon et al. 1988) result from Mie computations for homogeneous spheres, with the necessary assumptions concerning the (highly variable) refractive index of particles. Volume scattering functions (VSF) between 0.17° and 170° have been determined in three different water types by Petzold (1972), allowing extrapolation toward backscattering coefficients. In situ backscattering has been measured by Downing (1983) in highly turbid areas. More recently, Honey and Maffione (unpubl. data) derived backscattering coefficients from measurements of scattering in the angular range of 115–170° made in waters off southern California. However, simultaneous vertical profiles of backscattering, biomass, and seston concentration do not seem to exist; hence, variations in backscattering have not been analyzed with respect to the nature of particles.

Combined use of commercial instruments and new prototypes (developed at Sea Tech, Inc., and WET Labs, Inc.) has provided the first opportunity for simultaneous measurement of vertical profiles of in situ attenuation (at 488 and 660 nm), absorption (at 488, 676, 750 nm), and backscattering (at 488 nm), as well as stimulated fluorescence. These measurements were made off the Oregon coast under varying oceanographic conditions. As the inherent optical properties are never perfectly measured, preliminary corrections are necessary to retrieve "true" coefficients from the measured parameters.

Our main aim is to describe these procedures for deriving the inherent optical properties from the measured parameters. Examples of vertical profiles of these optical coefficients, obtained at three contrasting sites, help determine whether the values of these coefficients are consistent with the more routinely measured parameters (attenuation at 660 nm, fluorescence, pigment concentration) as measured in these areas and which supplementary information the new instruments could provide. Finally, as an additional test for the new instruments, we examine whether the total scattering coefficients, as derived from in situ attenuation and absorption, can be reproduced with a Mie scattering model, taking into account the measured particle size distributions and a range of realistic values for the refractive indices of particles. A list of notation and units is provided.

Methods

Measurements were performed during a cruise off the Oregon coast on the RV *Wecoma* (18 September–2 October 1991). Three stations with contrasting oceanographic conditions were sampled: an oligotrophic site in the central gyre (G: 41°34′N, 132°W), a mesotrophic nearshore site (N: 42°05′N, 125°50′W), and a turbid inshore site (I: 43°26′N, 124°39′W).

Stimulated in situ fluorescence as well as the beam attenuation coefficient at 660 nm were measured respectively with a Sea Tech fluorometer (Bartz et al. 1988) and a 25-cm-pathlength Sea Tech transmissometer (Bartz et al. 1978). Measurements were also made with prototype instruments developed at Sea Tech, Inc.: a transmissometer with a peak wavelength of 488 nm, three absorption meters with peak wavelengths of 488, 676, and 750 nm; and a backscatterometer operating at 488 nm (Table 1).

The absorption meters are modified transmissometers with 25-cm pathlength, in which a reflective tube has been added and the collimated receiver replaced by a large-area detector. A detailed description was given by Zaneveld et al. (1990, 1992) and (for an implemented version) Moore et al. (1992). The backscatterometer is a modified fluorometer that detects the light backscattered by the medium between 115 and 155°. A wideband blue filter before the detector prevents detection of light emitted by fluorescence. According to Oishi (1990), the partial backscattering coefficients measured in this angular range are proportional to the total b_b with maximum prediction errors ranging from 18% (at 140°) to 31% (at 150°) for various types of water.

Repetitive casts were made at each station (16 casts over 2 d at Sta. G; 15 casts over 3 d at Sta. N; 11 casts over 2 d at Sta. I). The attenuation coefficient at 660 nm and in situ fluorescence were measured simultaneously with pressure and temperature. The backscattering coefficient at 488 nm was measured for stations N and I only. Among the four other instrument configurations, only two could be used simultaneously for a given cast. Therefore, profiles of either $c(488)$ and $a(488)$, $a(488)$ and $a(676)$, or $a(676)$ and $a(750)$ were determined simultaneously.

The sensitivity of the fluorometer is ± 0.02 mg m^{-3} (equivalent Chl *a* units). The resolution of the transmissometers is $\pm 0.01\%$ in transmission (± 0.0005 m^{-1} for c varying in the range of 0.4–0.9 m^{-1} at 660 nm). The presence of large-area detectors in the absorption meters introduces some sensitivity degradation, the actual sensitivity being about $\pm 0.03\%$ in transmission (M. Borgerson pers. comm.) or ± 0.0015 m^{-1} in a.

The air calibration value of the red transmissometer as measured in the laboratory was lower than the factory calibration value by 0.34% (likely due to a decrease in the LED light output), and the measured transmission values were consequently corrected.

In the prototype transmissometer and absorption meters, the measured signals are internally temperature com-

Notation

λ	Wavelength, nm
a	Absorption coefficient, m^{-1}
c	Attenuation coefficient, m^{-1}
b	Scattering coefficient, m^{-1}
b_b	Backscattering coefficient, m^{-1}
a_m	Coefficient measured with the absorption meter, m^{-1}
c_m	Coefficient measured with the transmissometer, m^{-1}
Vb_b	Signal measured with the backscatterometer, V
a_w, c_w, b_w, b_{bw}	Optical coefficients of pure water, m^{-1}
b_{sw}	Scattering coefficient of pure seawater, m^{-1}
b_{bsw}	Backscattering coefficient of pure seawater, m^{-1}
b_p	Particulate scattering coefficient, m^{-1}
b_{bp}	Particulate backscattering coefficient, m^{-1}
T	Temperature, °C
α	Temperature dependence of $a_w(750)$, $m^{-1}(°C)^{-1}$
r	Optical pathlength of the instruments, m
ϵ	Acceptance angle of the detector in the absorption meter, degrees
ρ	Reflectivity of the silver coating in the absorption meter
k	Fraction of scattering detected in the absorption meter
a_y, a_{phy}, a_{nc}	Absorption coefficient of yellow substance, living algal cells, and non-chlorophyllous particles, m^{-1}
a_{bl}, b_{bl}	Optical coefficients of the algal bloom, m^{-1}
$Q_{i,bl}$	Efficiency factors of the algal bloom
a_{op}, b_{op}	Optical coefficients of particles (bloom excluded), m^{-1}
$Q_{i,op}$	Efficiency factors of particles (bloom excluded)
$n_{bl} - in'_{bl}$, $n_{op} - in'_{op}$	Complex refractive index of algal cells in the bloom and of other particles
D	Equivalent sphere-diameter of a particle, μm
N/V	Particle number per unit of volume, ml^{-1}

pensated. The resulting temperature stability is better than $\pm 0.1\%$ in transmission, or ± 0.005 m^{-1} in c or a, over a range of 0–25°C. For all the other devices (fluorometer, red transmissometer, backscatterometer, and pressure and temperature sensors), the variations in signals induced by temperature changes in the A/D converter were corrected by using a reference voltage recorded simultaneously.

A differential filter has been applied to the measured signals to remove the electronic spikes. The profiles have not been further smoothed to prevent the loss of the actual small-scale variability in the signals. No correction for the response time of the different devices was applied because the upcasts reproduced the downcasts with a depth shift of <2–3 m.

Supplemental measurements included fluorometrically determined chlorophyll *a* and pheophytin *a* concentrations from water samples passed onto GF/F filters and cold extracted for 24 h in 90% acetone. Particle size distributions were obtained with a Coulter Counter using 30- and 100-μm apertures. Particulate absorption spectra were measured spectrophotometrically on GF/F filters according to Roesler et al. (1989). Absorption coefficients were calculated with a spectrally dependent pathlength amplification factor (Roesler and Perry unpubl. data).

Calibration of attenuation and absorption in absolute values—Each instrument provides transmission values multiplied by a constant calibration factor (K) to be determined. The transmissometer operating at 660 nm was previously calibrated with filtered water. The transmissometer operating at 488 nm and the three absorption meters were calibrated by measuring the transmission values (KT) in optically pure water, supplied by a reverse-osmosis filtration system (C. Moore pers. comm.). Although the absorption spectra of distilled and reverse osmosis water are very similar for wavelengths longer than 640 nm, those of reverse-osmosis water are considerably lower in the blue and green parts of the spectrum (Zaneveld et al. 1990). For each device, the calibration factor has been obtained by converting the measured transmission into an attenuation or absorption coefficient:

$$c \text{ (or } a) = -(1/r) \ln(KT) = -(1/r) \ln T - (1/r) \ln K$$

Table 1. List of the parameters measured at each wavelength and of the corresponding optical coefficients as derived using the procedures outlined in Fig. 3. G, N, and I indicate that successful measurements have been performed (and optical coefficients have been derived) at the gyre, nearshore, and inshore stations.

	Measured optical parameters			Derived optical coefficients				
λ (nm)	a_m	c_m	Vb_b	a	c	b	b_b	b_b/b
488	GNI	GNI	NI	GNI	GNI	GNI	NI	NI
660		GNI			GNI			
676	NI			NI				
750	NI			NI				

(where $r = 0.25$ is the pathlength in m), setting c or a to that of pure water, and solving for K.

The values of a of pure water used in this study are those determined by Tam and Patel (1979), namely $a_w(488) = 0.019$ m^{-1} and $a_w(676) = 0.408$ m^{-1}. Their measurements, however, did not extend beyond 700 nm. In the infrared region, relative values of a have been measured by Pegau and Zaneveld (1993) and converted to absolute values by adjusting $a_w(685)$ to the value determined by Tam and Patel (1979). Pegau and Zaneveld identified a strong temperature effect between 730 and 775 nm. The absorption coefficient resulting from their study is $a_w(750) = 2.678$ m^{-1} at 21°C (the temperature at which the calibration was performed).

Note that the computation of $(a - a_w)(750)$ requires accounting for the dependence of $a_w(750)$ on temperature, by means of the relationship

$$(a - a_w)(750) = a(750) - 2.678 - \alpha(21 - T) \quad (1)$$

where T is in °C. From spectrophotometric measurements, α has been found to be close to 0.009 m^{-1} °C^{-1} (Pegau and Zaneveld 1993). The actual value for the absorption meter (which may be slightly different because of the instrument bandwidth) has been adjusted (by trial and error on the field data) to 0.010 m^{-1} °C^{-1}. This necessary correction has been eliminated in the improved version of the absorption meter (Moore et al. 1992) by shifting the peak wavelength from 750 to 712 nm, where there is virtually no temperature dependence (Pegau and Zaneveld 1993).

The attenuation coefficients for pure water (c_w) at 488 and 660 nm are obtained by summing the absorption (a_w) and scattering (b_w) coefficients at the corresponding wavelengths, the latter as provided by Morel (1974), which leads to $c_w(488) = 0.022$ m^{-1} and $c_w(660) = 0.371$ m^{-1}. The value of $c_w(660)$ is very close to that previously used (0.364 m^{-1}) for the factory calibration of the transmissometer. For consistency, we kept this latter value and used a value of 0.363 m^{-1} for $a_w(660)$.

Note that the actual values of c_w and a_w differ by a few percent from the above coefficients because of the instrument bandwidth [40 nm for $c(660)$, 10 nm for the other parameters]. This error, however, affects the total coefficients, but not the nonwater coefficients discussed later.

Correction of absorption and attenuation coefficients for the scattering contribution—The measurements performed with a transmissometer provide an underestimated value of c because a small amount of forward scattered light is unavoidably received by the detector. Given the detector acceptance angle (0.9°) in the Sea-Tech transmissometers, Zaneveld et al. (1992) found that the difference between the actual and measured attenuation coefficients ($c - c_m$) is 4–10% of the total b for various volume scattering functions, i.e.

$$c = c_m + 0.07(\pm 0.03)b. \quad (2a)$$

Here we have adopted the mean value of 0.07. Using this value leads to an uncertainty of $\pm 0.03b$, i.e. (because $c > b$) <3% on the corrected c value.

Ideally, the detector of the absorption meter should be able to collect all directly transmitted light as well as forward scattered light and then to provide a measurement of $a + b_b$ (with $b_b \ll a$). However, because of both the imperfect reflectivity of the quartz-silver tube wall and the limited acceptance angle of the detector, photon losses are, in practice, much higher, and the measured absorption coefficient (a_m) overestimates the actual a. Kirk (1992), using a Monte-Carlo model, has shown that the error in measuring "true" absorption ($a_m - a$) is a linear function of b:

$$a_m = a + kb \quad (2b)$$

with the slope k determined by both the VSF of waters, the acceptance angle of the detector (ϵ), and the reflectivity (ρ) of the silver coating. For $\epsilon = 70°$ and $\rho = 0.94$ (the tube reflectivity estimated by Zaneveld et al. 1990) and for the VSF measured by Petzold (1972), k ranges on average from 0.15 for a turbid coastal water to 0.21 for a clear oceanic water. This value is extremely sensitive to variations in ρ, dropping to <0.04 for $\rho = 1$. With these ϵ and ρ values, Zaneveld et al. (1990) obtained k values between 0.07 and 0.13 for various size distribution functions and refractive indices (i.e. for various VSF).

Because uncertainty remains on both the exact value of the tube reflectivity and the actual VSF, we preferred an empirical approach using the infrared absorption measurements. At 750 nm, the nonwater a is very weak compared to b, and the retrieved absorption values are highly sensitive to the applied correction. This correction was adjusted by trial and error to fulfill the following criteria: $0 < (a - a_w)(750) < (a - a_w)(676)$ (within experimental uncertainty); no inverse relationship between $(a - a_w)(750)$ and $c(660)$, which would indicate an overcorrection [a subsurface maximum is expected, as for $c(660)$ and $a(676)$]. A value of $k = 0.05$ was found to best fulfill these conditions at the nearshore station (Fig. 1). According to Kirk (1992), this value is compatible with a reflectivity of 0.98—higher than the value previously assumed but corresponding to the manufacturer's specification for the reflective tube. Considering the spectral variations in silver reflectance (Am. Inst. Physics 1972), we estimated that the reflectivity of the tube (virtually unchanged at 676 nm) drops to 0.966 at 488 nm, which leads to $k = 0.08$ at that wavelength. Keep in mind that k is expected to fluctuate slightly with the particle population and, therefore, with the water type (Kirk 1992) and depth (Zaneveld et al. 1992).

To retrieve a and c, given a value of k, simultaneous measurements of absorption (a_m) and attenuation (c_m) are desirable. In such a case, the system of Eq. 2 can be solved as

$$c = [(1 - k)c_m - 0.07a_m]/(0.93 - k) \quad (3a)$$

$$a = (0.93a_m - kc_m)/(0.93 - k). \quad (3b)$$

Simultaneous measurements of $a_m(488)$ and $c_m(488)$ were performed at each station, and Eq. 3a and b (with $k = 0.08$) were applied to retrieve $a(488)$ and $c(488)$ for the corresponding casts. For those casts where only $a_m(488)$

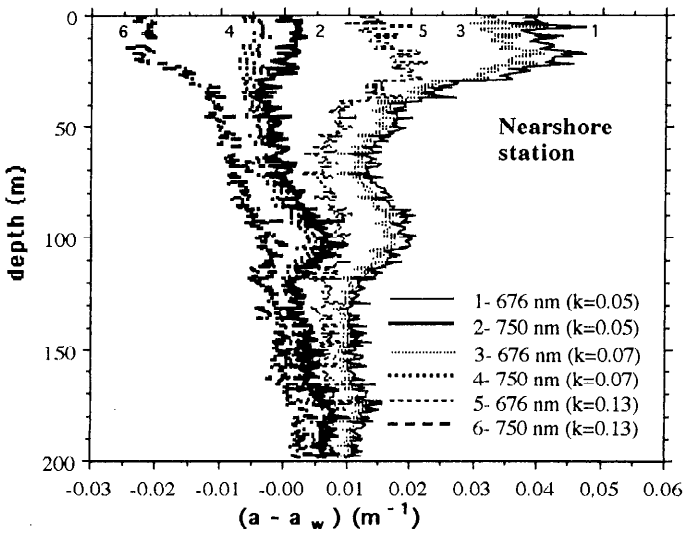

Fig. 1. Vertical profiles of the nonwater absorption coefficients at 676 and 750 nm corrected for scattering, for different values of k (*see Eq. 2b*). The profiles for 676 and 750 nm are shown by thin lines and thick lines, respectively. The uncertainty in the absolute value of $(a - a_w)(750)$, due to correction of the temperature dependence of $a_w(750)$, is ~0.010 m^{-1} near the surface and 0.014 m^{-1} in deep waters.

was available, $c(488)$ was derived from $c(660)$. Simultaneous determinations of $c(488)$ and $c(660)$ at each site demonstrate that a linear relationship exists between both coefficients (Fig. 2), with a slope ranging from 1.19 at station N to 1.32 at station G (or, if a law in λ^{-n} is assumed, n ranging from 0.6 to 0.9). These slopes bracket well that obtained (1.24) with the empirical relationship describing the spectral variation of $(c - c_w)$ established by Voss (1992) for both oceanic and coastal waters. $a(488)$ was then retrieved from $a_m(488)$ and $c(488)$ by means of Eq. 2b (with $b = c - a$).

In the absence of absorption measurements at 660 nm, $c_m(660)$ was corrected by assuming that $b_p(660) \approx (c - c_w)(660)$ [or equivalently $b_p(660) \gg (a - a_w)(660)$]. Therefore, $b(660) \approx c(660) - a_w(660)$, and, according to Eq. 2a,

$$c(660) \approx c_m(660) + 0.07[c(660) - a_w(660)],$$

or

$$c(660) \approx 1.075c_m(660) - 0.075a_w(660). \quad (4)$$

Note that the <5% error affecting $a_w(660)$, due to instrument bandwidth, results in an insignificant (<0.0014 m^{-1}) error on $c(660)$.

Finally, because no attenuation measurements at 676 and 750 nm were available, $a_m(676)$ and $a_m(750)$ were corrected with Eq. 2b (with $k = 0.05$), where $b(676)$ and $b(750)$ were extrapolated from $c(660)$. In the absence of experimental data concerning the spectral dependence of b or c in the red-infrared part of the spectrum, it was stated (as previously) that $b_p(660) \approx (c - c_w)(660)$, and b_p was assumed to vary as λ^{-1}.

The correction procedures are summarized in Fig. 3.

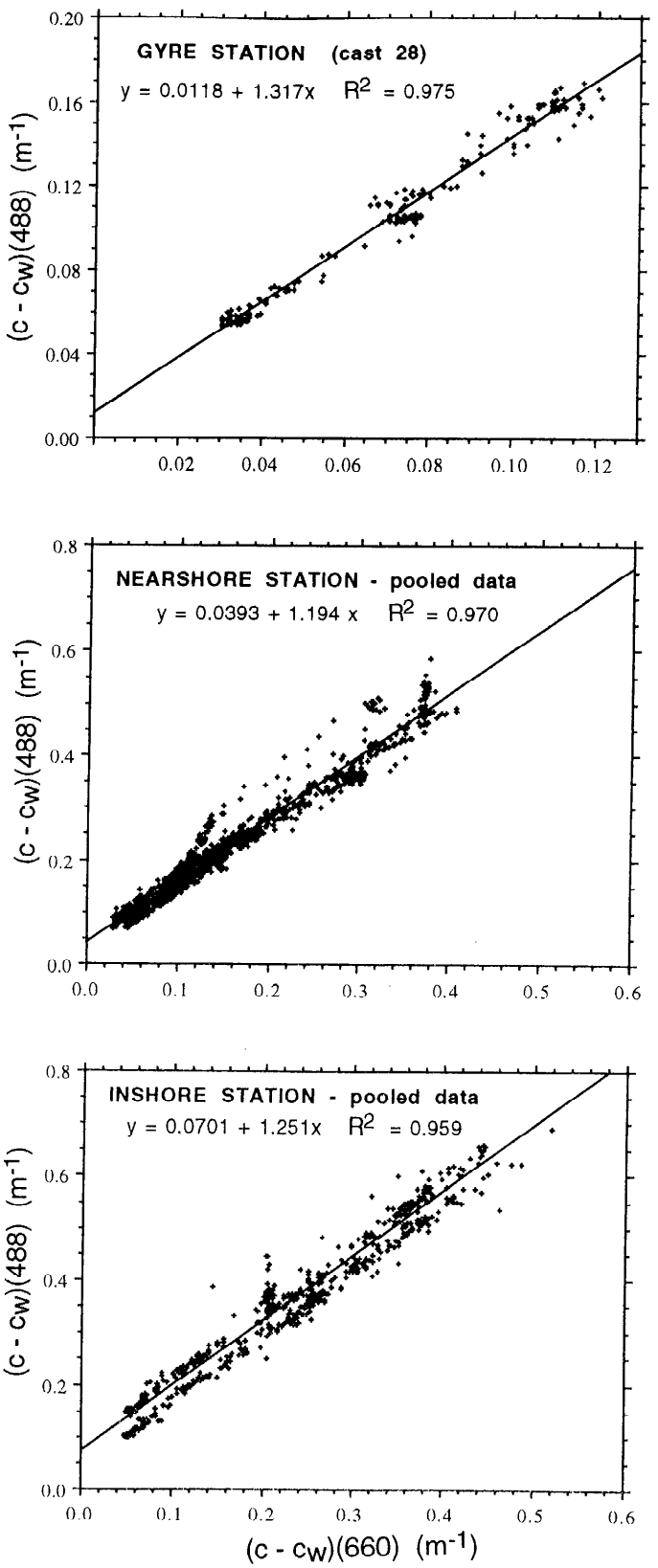

Fig. 2. Nonwater attenuation coefficient $(c - c_w)$ at 488 nm as a function of the same coefficient at 660 nm, at the three stations.

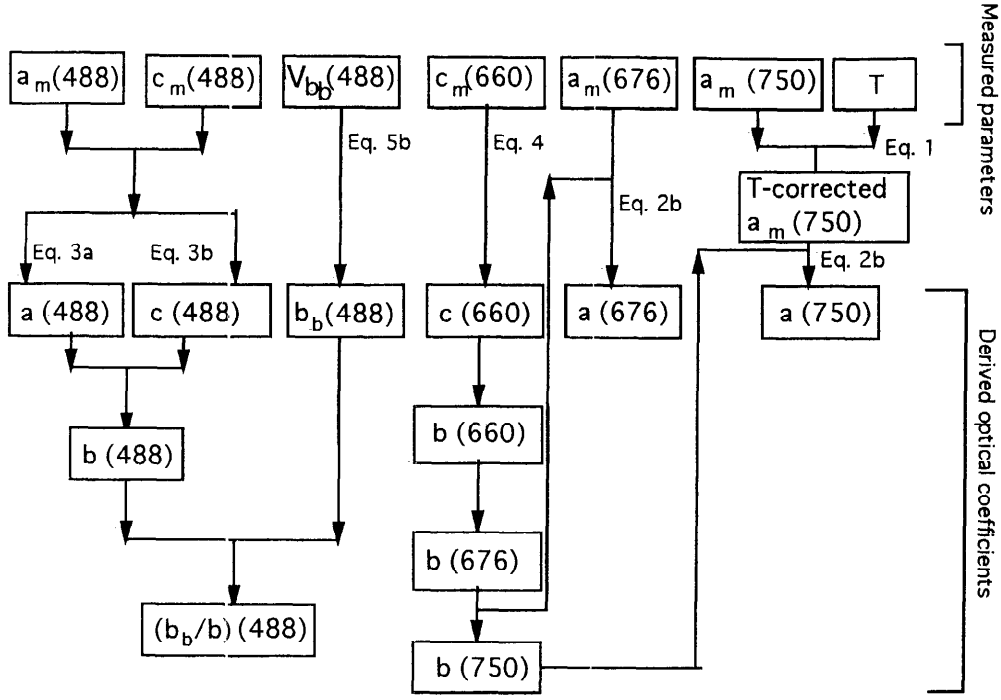

Fig. 3. Flowchart of the correction procedures for extracting the "true" optical coefficients from the measured parameters. When $c_m(488)$ has not been measured simultaneously with $a_m(488)$, $c(488)$ is derived from $c(660)$ using a statistical relationship (*see Fig. 2*). $b(660)$ is taken equal to $c(660) - a_w(660)$. $b(676)$ and $b(750)$ are computed assuming that $(b - b_{sw})(\lambda)$ varies according to a spectral law in λ^{-1}.

Figure 4, where uncorrected and corrected values of $c(488)$, $a(488)$, $a(676)$, and $a(750)$ are displayed as examples, demonstrates that although the scattering correction remains weak for c, it is critically important for a at all three wavelengths due to the high $b : a$ ratios encountered. Figure 4c and d, however, shows that the assumption concerning the spectral dependence of b_p has a negligible effect on the retrieved values of $a(676)$ and $a(750)$. The most critical factor for determining accurate absorption coefficients appears to be the actual spectral values of k and their possible fluctuations induced by changes in the tube reflectivity or in the VSF (the latter stemming, in turn, from changes in the particle refractive index or size distribution).

Note that if the complex procedures described above remain fully applicable to Sea Tech absorption meters, most of the problems are circumvented in the improved version of the instrument developed by Moore et al. (1992). The quartz-silver tube is replaced by a clear quartz tube (using the internal reflection principle); therefore the spectral reflectivity is much more easily controlled and does not degrade over time. In addition, estimating the spectral variation of the scattering contribution will be greatly aided by simultaneously determining a and c at multiple wavelengths.

Note that the scattering contribution has not been taken into account when calibrating the different instruments with pure water. Although the resulting relative error is negligible for c (due to the absence of a forward scattering peak), it can be approximated by b_{bw}/a_w or $b_w/2a_w$ for absorption, which gives 6, 0.06, and <0.01% for $a(488)$, $a(676)$, and $a(750)$.

Calibration of backscattering measurements in absolute values—The ratio of the backscattered flux (Fb_b) to the incident flux (F_0) can be expressed as

$$Fb_b/F_0 = [1 - \exp(-b_b r)]\exp(-2cr).$$

The first term in this equation represents the part of the incident flux that would be backscattered if attenuation were negligible in the sample, and the second term accounts for attenuation of the light beam when crossing the sample twice. The exact value of r is unknown due to the geometrical configuration but is <0.1 m. Even at station I, $c(488)$ and $b_b(488)$ remain lower than 0.7 and 0.01 m^{-1} (*see later*); consequently $2cr \ll 1$ and $b_b r \ll 1$. The measured signal (Vb_b) is proportional to $Fb_b : F_0$; therefore

$$Vb_b \approx Kb_b r \exp(-2cr) \quad (5a)$$

or

$$b_b \approx K' Vb_b. \quad (5b)$$

Thus, b_b is proportional to the measured signal. because $r < 0.1$ m, the variable term introduced by attenuation of the light beam, $\exp(-2cr)$, is >0.87 in the most turbid waters encountered during this cruise and >0.98 in the clearest waters.

A calibration of the backscatterometer (i.e. a determination of the constant K') is hardly achievable in the

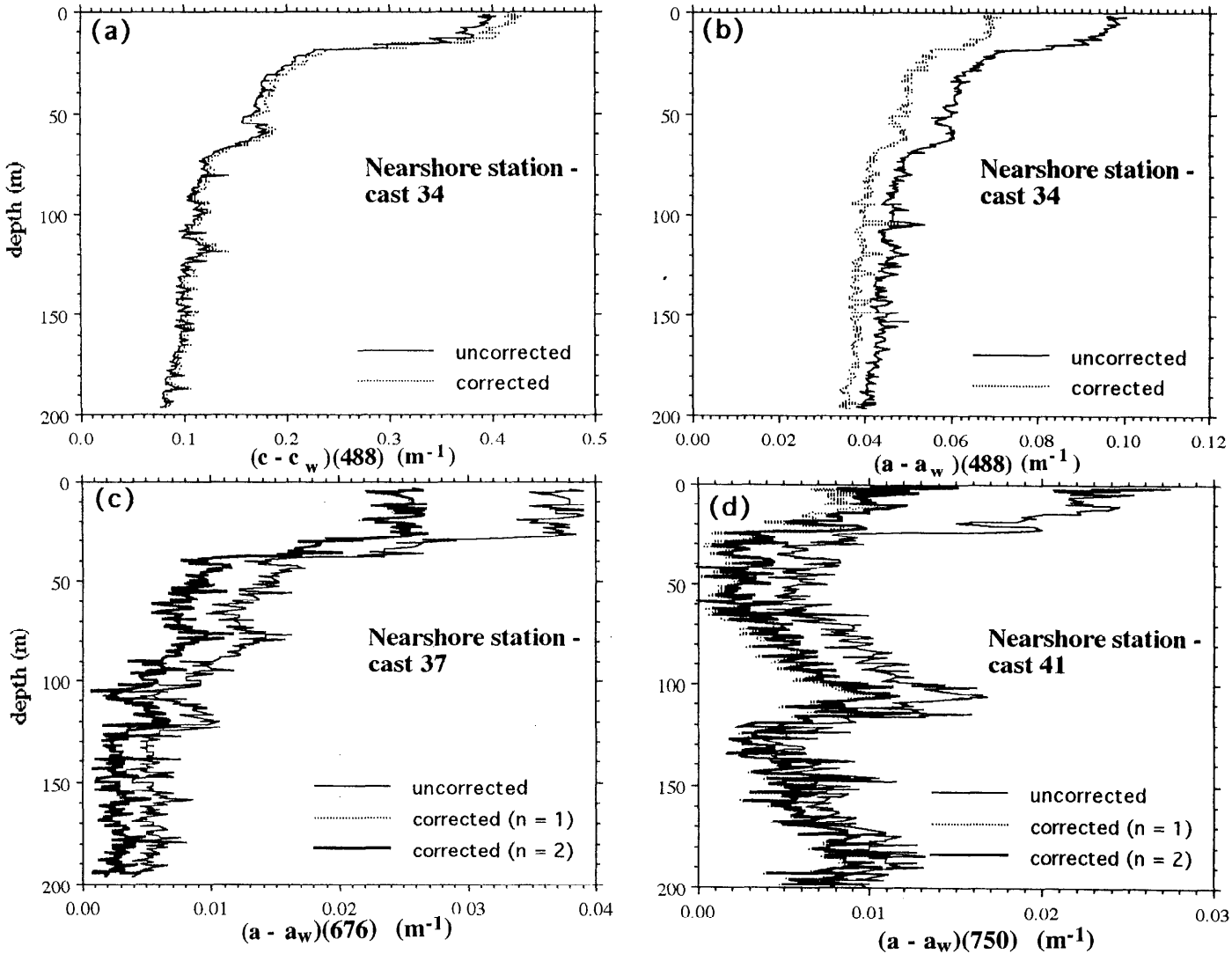

Fig. 4. Vertical profiles of the nonwater attenuation coefficient at 488 nm (a), the nonwater absorption coefficients at 488 nm (b), 676 nm (c), and 750 nm (d) before and after correction for the scattering contribution. The corrected values of $c(488)$ and $a(488)$ were obtained with Eq. 3a,b (with $k = 0.08$). Those of $a(676)$ and $a(750)$ were obtained with Eq. 2b (with $k = 0.05$) with the scattering coefficients $b(676)$ and $b(750)$ computed from $c(660)$, assuming that particulate scattering, b_p, varies as λ^{-n}, where $n = 1$. The profiles obtained for an exponential coefficient of $n = 2$ (shown as thick lines) are practically indistinguishable from those corresponding to $n = 1$ (dotted lines).

laboratory because reflections on the inside walls of the tank are difficult to eliminate. Furthermore, in the blue part of the spectrum, b (or b_b) is much more sensitive than a or c to small impurities possibly present in water. We therefore attempted to perform an empirical calibration by analyzing the relationships between $Vb_b(488)$ and $(c - c_w)(660)$, as observed at stations N and I (Fig. 5). There seems to be a significant correlation between both parameters, although there are site- and depth-specific trends (*see below*). When extrapolating the observed relationships to $(c - c_w)(660) = 0$, an approximate value of Vb_b for pure seawater (0.13 ± 0.02) is obtained. Combining this value with that of $b_b(488)$ for pure seawater ($b_{bsw} = 0.0015$ m^{-1}, Morel 1974) leads to $K' = 0.0115$, with ~20% uncertainty. This rough calibration does not take into account possible multiple scattering effects, however the quasi-linear variations of $Vb_b(488)$ with $(c - c_w)(660)$, especially for high seston concentrations, suggest that these effects remain weak in the range of variation experienced by $b_b(488)$.

The relative uncertainty of K' is integrally transferred to $b_b(488)$ (*see Eq. 5b*). Therefore, when b_{bp} ($= b_b - b_{bsw}$) is computed, the relative uncertainty of this coefficient dramatically increases when it becomes lower than b_{bsw} (close to 40% for 1.5×10^{-3} m^{-1} or 100% for 3×10^{-4} m^{-1}). Consequently, $b_{bp}(488)$ values lower than $\sim 10^{-3}$ m^{-1} should be considered qualitatively. Unless a more accurate calibration can be performed and the instrumental noise decreased, obtaining reliable values of b_b in clear oceanic waters with this device is limited.

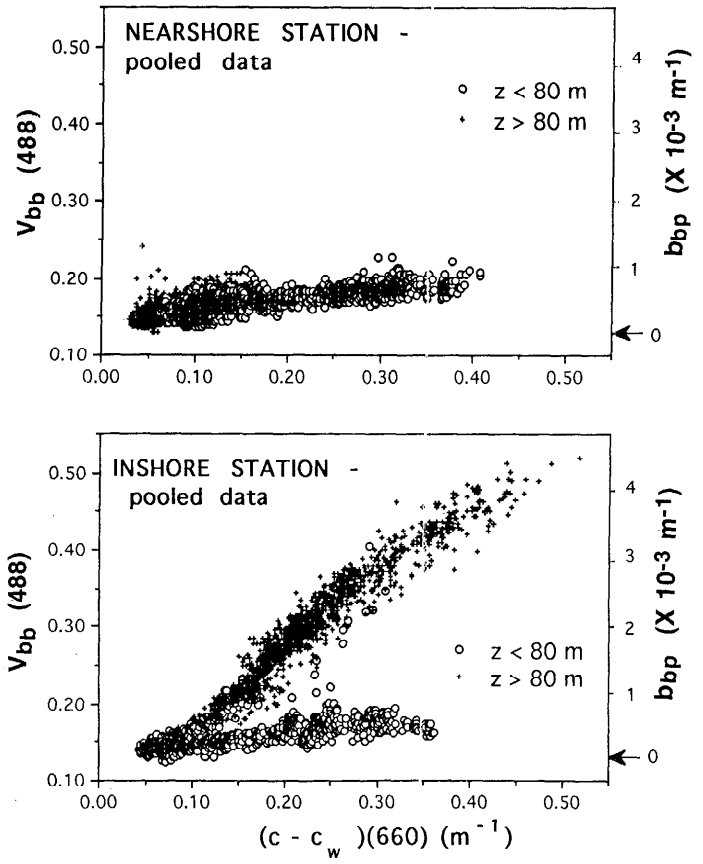

Fig. 5. Measured backscattering signal, $Vb_b(488)$ (in arbitrary units), as a function of the nonwater attenuation coefficient $(c - c_w)$ at 660 nm, at the nearshore and the inshore stations.

Computation of the particulate optical coefficients—When removing the contribution of pure seawater from the attenuation and absorption coefficients measured in situ, we used the set of coefficients for pure water because the increase of absorption due to dissolved salts is essentially confined to the UV region. The scattering coefficients of pure seawater are ~30% higher than those of chemically pure water (Morel 1974). Although the effect on $c_w(488)$ and $c_w(660)$ is negligible, this increase must be taken into account when dealing with the in situ particulate scattering $[b_p(488)]$ or backscattering $[b_{bp}(488)]$ coefficients. These must be computed by subtracting the coefficients for pure seawater (b_{sw} and b_{bsw}) from the total coefficients.

Results and discussion

Characterization of the sampled sites—Although the relationship between in vivo fluorescence and Chl *a* concentration is known to be affected by environmental and physiological variables (e.g. Cullen et al. 1988), the general distribution of phytoplankton can, in principle, be tracked from stimulated in situ fluorescence. The beam attenuation coefficient at 660 nm has been demonstrated to be well correlated to total suspended seston concentration (e.g. Gardner at al. 1985; Pak et al. 1988). Therefore, the vertical variations of attenuation and fluorescence allow the sampled sites to be characterized with respect to their distributions of phytoplankton and total seston.

At the gyre station (Sta. G, Fig. 6a), the fluorescence profiles showed a distinct vertical structure with a sharp deep maximum around 80–85 m. The attenuation profiles displayed similar but less variable patterns, with the maximum often shifted 10–15 m toward the surface with respect to the fluorescence maximum, indicating a lack of coherence between the distribution of chlorophyll and the distribution of total seston (Kitchen and Zaneveld 1990).

At the nearshore site (Sta. N, Fig. 6b), although the fluorescence intensity exhibited some temporal variability, the vertical variations showed reproducible patterns between casts, with a thick maximum at 10–20-m depth, a sharp decrease at 30–40 m, and a series of weaker maxima at greater depths. Vertical profiles of in situ fluorescence and *c* at 660 nm (or 488 nm) were well correlated, except on some occasions near the surface where fluorescence may be inhibited.

The inshore site (Sta. I) was characterized by a much larger temporal variability in the vertical profiles of both fluorescence and beam attenuation. On the first day (30 September, cast 46, Fig. 6c), fluorescence exhibited a strong maximum around 30 m and only one secondary maximum at ~90 m. The maximum around 30 m migrated toward the surface in later casts. Beam attenuation and fluorescence covaried in the 0–90-m layer. At greater depths, however, fluorescence declined but *c* increased, reaching values ~5-fold higher than those in the deep layer of station N. On the second day (1 October, cast 52, Fig. 6d), fluorescence and, to a lesser extent, beam attenuation exhibited lower values than on the previous day, and a sharp maximum in attenuation appeared at 90–100 m (progressively increasing in intensity). A clearer water layer was found at ~110 m. The fluorescence and attenuation profiles showed little covariance. The high attenuation coefficients observed in the deep layer were very likely due to resuspension of sediments near the coast because the depth of the bottom was <250 m. A 3-d storm with winds >15 m s^{-1} occurred the previous week.

Simultaneous values of particulate scattering at 488 nm $[b_p(488)]$ and fluorescence were compared for stations I and N with a view to identifying them as oceanic-Case 1 or turbid-Case 2 waters. The criterion defined by Morel (1980) to delineate Case 2 waters,

$$(b_p + b_{sw})(546) > 0.42C^{0.62},$$

was transformed by extrapolating b_p from 546 to 488 nm (assuming a λ^{-1} spectral dependence) and by converting the pigment concentration *C* (Chl *a* + pheophytin *a*) into fluorescence with piecewise regressions between measured pigment concentrations and fluorescence for each cast (or the temporally closest cast). This comparison shows that waters in the nearshore site were unambiguously Case 1 (Fig. 7a), and thus contained insignificant concentrations of mineral particles. Even in the inshore site (Fig. 7b,c), the waters from the upper layer (with

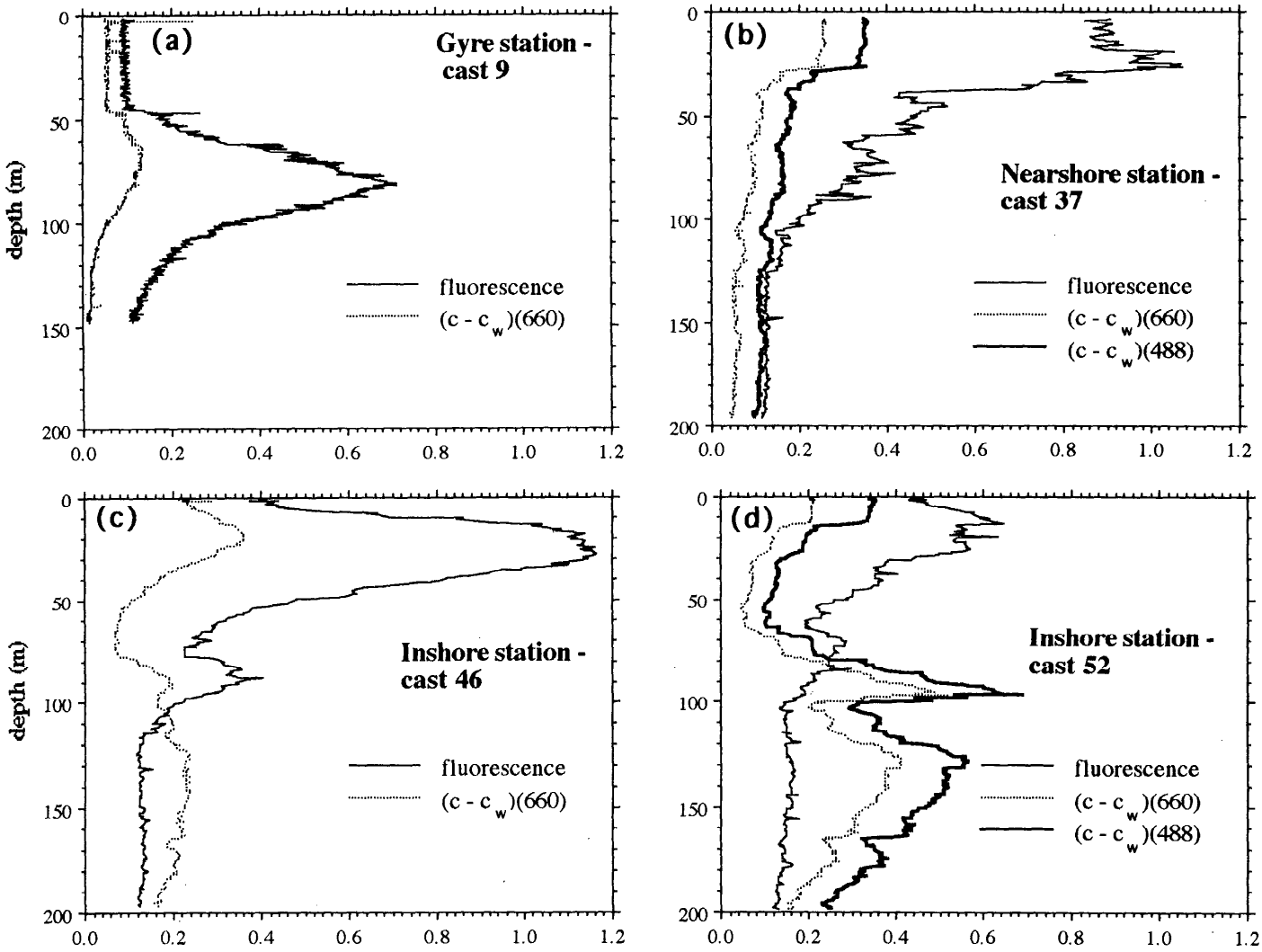

Fig. 6. Typical vertical profiles of fluorescence (in arbitrary units) and of the nonwater attenuation coefficients ($c - c_w$) at 660 and (when available) 488 nm (m^{-1}), for the three stations.

fluorescence values >0.20–0.25) remained below the Case 1 limit, and the mineral particles seemed to be confined mostly to the deep layer (>100 m on the first day, >60 m on the second day).

Vertical variations of the absorption coefficients at 488 and 676 nm and of the red-to-blue absorption ratio—Vertical profiles of absorption and fluorescence covary throughout the water column at all stations, except in the deep layer at station I (Figs. 6 and 8). Both $(a - a_w)(488)$ and $(a - a_w)(676)$ exhibit maxima that track the fluorescence maxima. At station G (Fig. 8a), $(a - a_w)(488)$ decreases sharply below the maximum at 80 m and tends to stabilize around 0.025 m^{-1} in the deep layer [a reliable measurement of $a(676)$ was not available at this station]. At station N, the value of $(a - a_w)(676)$ is very low (0.002–0.006 m^{-1}) at depths >50 m, coincident with decreased fluorescence, whereas $(a - a_w)(488)$ is approximately constant (~0.06 m^{-1}) (Fig. 8b). In the deep layer at station I, the value of $(a - a_w)(676)$ is larger (~0.03 m^{-1}), coincident with a factor of five larger $c(660)$ (*see Fig. 6c*). The $(a - a_w)(488)$ values, however, remain similar to those at station N (Fig. 8c). In this deep nepheloid layer, some uncertainty exists on the absorption coefficients because the particles present in this layer likely differ in their optical properties from those in the surface layer; therefore k may be different. According to Kirk (1992), k is lower in coastal turbid waters than in oceanic waters; therefore, the increase of absorption in this layer is thought to be real (and not due to an undercorrection of absorption).

The in situ measured absorption can be split into the contributions of three main components beside that of pure seawater (a_w): living algal cells (a_{phy}), nonchlorophyllous particulate matter (a_{nc}), and dissolved yellow substance (a_y). a_{nc} includes both detrital and living biogenous particles and, in turbid-Case 2 waters, mineral particles. Heterotrophic organisms such as bacteria and microzooplankton have a spectral absorption signature very similar to that of detrital particles (Morel and Ahn

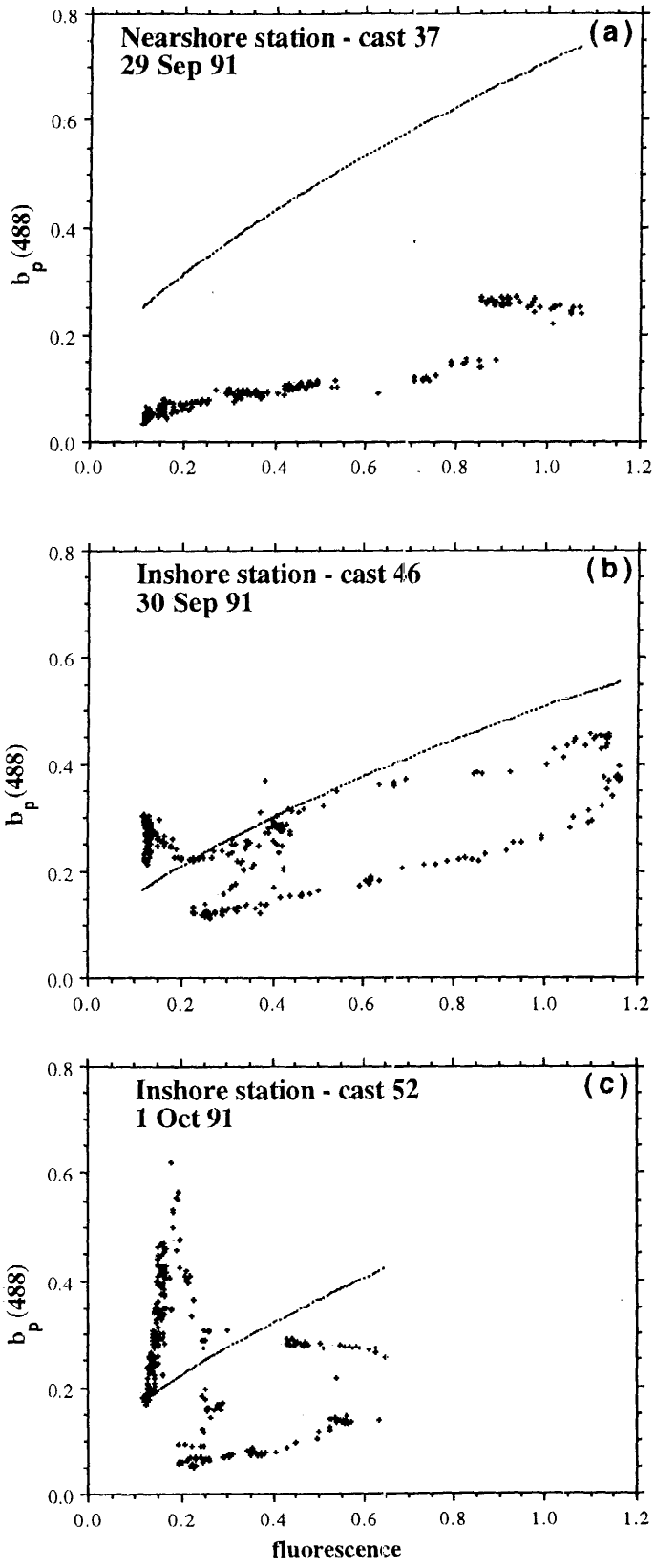

Fig. 7. Relationship between the particulate scattering coefficient (b_p) at 488 nm (in m^{-1}) and fluorescence (in arbitrary units) at the nearshore and inshore stations. Dotted lines indicate the demarkation between oceanic-Case 1 waters and turbid-Case 2 waters as defined by b(550) and pigment concentration (Morel 1980). The transformation from b_p(550) to b_p(488) assumed a spectral dependence of λ^{-1}; the transformation from pigment concentration to fluorescence was determined from discrete samples collected for the same (or temporally closest) cast.

1990, 1991), as do macrozooplankton (Roesler unpubl. data), which conveniently groups them optically.

Because of the variability of the absorption spectral signatures by the different substances, we do not have a straightforward way to check the amplitude of the in situ absorption coefficients as a function of the substance concentrations. The most direct way would be to compare in situ absorption to the sum of absorptions by particulate matter (i.e. $a_p = a_{phy} + a_{nc}$) and dissolved organics (a_y) as measured separately on discrete samples. Because of the absence of measured a_y spectra, only the particulate absorption profiles were compared to the closest in situ absorption profiles. The particulate absorption profiles covary with the in situ absorption profiles, exhibiting the same subsurface maxima at both stations N (not shown) and I (Fig. 9), decreasing at the same rate below this maximum and then, at station I, showing a similar trend to increase at the top of the deep turbid layer. As a consequence, the difference between in situ and particulate absorptions attributable to dissolved organics exhibit reasonable amplitude and vertical patterns. a_y is relatively stable, varying within a factor of <2. The amplitude of $a_y(488)$ (~0.03–0.07 m^{-1} at Sta. N, 0.03–0.05 m^{-1} at Sta. I) falls in the range encountered for oceanic waters (Bricaud et al. 1981). $a_y(676)$, which is expected to be much lower than $a_y(488)$, appears overestimated (Fig. 9b), likely resulting from combined errors in $a_p(676)$ (uncertainty in the pathlength amplification factor, higher at 676 nm than at 488 nm) and in $(a - a_w)(676)$ (uncertainty in the scattering correction). That the retrieved profiles of a_y do not show systematic correlation with the corresponding attenuation profiles and, in particular, do not exhibit the same large maximum near the surface (Fig. 6b,c,d) suggests, however, that the in situ absorption profiles have not been undercorrected (i.e that the contribution of scattering to the measured values has not been underestimated).

The reliability of the in situ absorption values can also be evaluated by examining the height of the red absorption peak of phytoplankton, as approximated by the difference $(a - a_w)(676) - (a - a_w)(750)$ (it is actually slightly lower than this term, because absorption by detrital matter is increasing toward shorter wavelengths). The variation range of the height of this peak in natural waters is 0.010–0.020 m^2 mg^{-1} (Bricaud and Stramski 1990; unpubl. data) with a theoretical maximal value of 0.021 m^2 mg^{-1} (attainable in absence of package effect). For the small set of simultaneous pigment concentrations, $(a - a_w)(676)$ and $(a - a_w)(750)$ data (only two casts), the slopes of the regression curves of $(a - a_w)(676) - (a - a_w)(750)$ vs. (Chl a + pheo a) concentrations (0.020 and 0.017) fall in the expected range. The corresponding cor-

relation coefficients (0.87 and 0.76) are significantly higher than those for the fluorescence vs. pigment concentration regression analysis (0.80 and 0.67). Although more analysis is necessary, these results suggest that the height of the red absorption peak may be a more reliable proxy measurement than is fluorescence for the determination of pigment concentration (*see* Moore et al. 1992).

The red-to-blue absorption ratio, $(a - a_w)(676):(a - a_w)(488)$, exhibiting large variations from surface to depth (Fig. 8), indicates changes in the relative concentrations of chlorophyllous (phytoplankton) and nonchlorophyllous (detrital) particles. This ratio may also provide information on the spectral behavior of absorption by the dominant particles. In the deep layer, where fluorescence reaches its minimum value and becomes stable ($z > 100$ m at Sta. N, 130 m at Sta. I), the pigment concentration can be assumed to be negligible with respect to the detrital matter concentration, and $a_{ph} \approx 0$. Therefore, $(a - a_w)(676):(a - a_w)(488)$ is about equal to $(a_y + a_{nc})(676):(a_y + a_{nc})(488)$. Absorption by yellow substance has been found to vary according to the spectral law:

$$a_y(\lambda) = a_y(\lambda_0)\exp[-S\,(\lambda - \lambda_0)]$$

where S ranges between 0.010 and 0.020 nm^{-1} (Bricaud et al. 1981; Carder et al. 1989). Particulate detrital matter appears to absorb light according to a similar spectral law (Yentsch 1962; Kirk 1980), with S in the range of 0.002–0.015 nm^{-1} (Roesler et al. 1989; Bricaud and Stramski 1990). The red-to-blue absorption ratios observed in the deep layer at station N (*see Fig. 8*) result in $S = 0.010$–$0.016\ nm^{-1}$, consistent with published values. In the deep layer at station I, the ratio is 5-fold–10-fold higher, and consequently S is much lower ($0.004\ nm^{-1}$). Considering that yellow substance contributes to this spectral dependence, this result suggests that the predominantly mineral particles present in the deep layer at station I absorb light relatively independent of wavelength.

Within the layer of the biomass maximum, particulate absorption spectra usually resemble those of pure phytoplankton, and the detritus-to-total absorption ratio is minimal (e.g. figure 15 of Bricaud and Stramski 1990). Consequently, the effect of detrital particles, although never negligible, is likely weakest near the fluorescence maximum, and the red-to-blue absorption ratio is closest to that of living algal cells. This ratio is expected to be variable for living phytoplankton as a result of both changes in species composition (i.e. pigment composition and size) and photoadaptation (e.g. Mitchell and Kiefer 1988). With the filter-pad technique, average values of 0.25 and 0.37 have been observed for the surface and deep layers in the Sargasso Sea and 0.47 in the Peru upwelling area, mainly due to an increasing package effect from the first to the third situation (Bricaud and Stramski 1990). This effect induces a flattening of the absorption spectrum (this flattening becomes more and more pronounced when cells become larger or more absorbing) (Kirk 1975; Morel and Bricaud 1981) and increases the red-to-blue ratio. The absorption ratios observed here in the vicinity of the fluorescence maximum range from 0.27 to 0.40 at station N and 0.40 to 0.50 at station I. Such

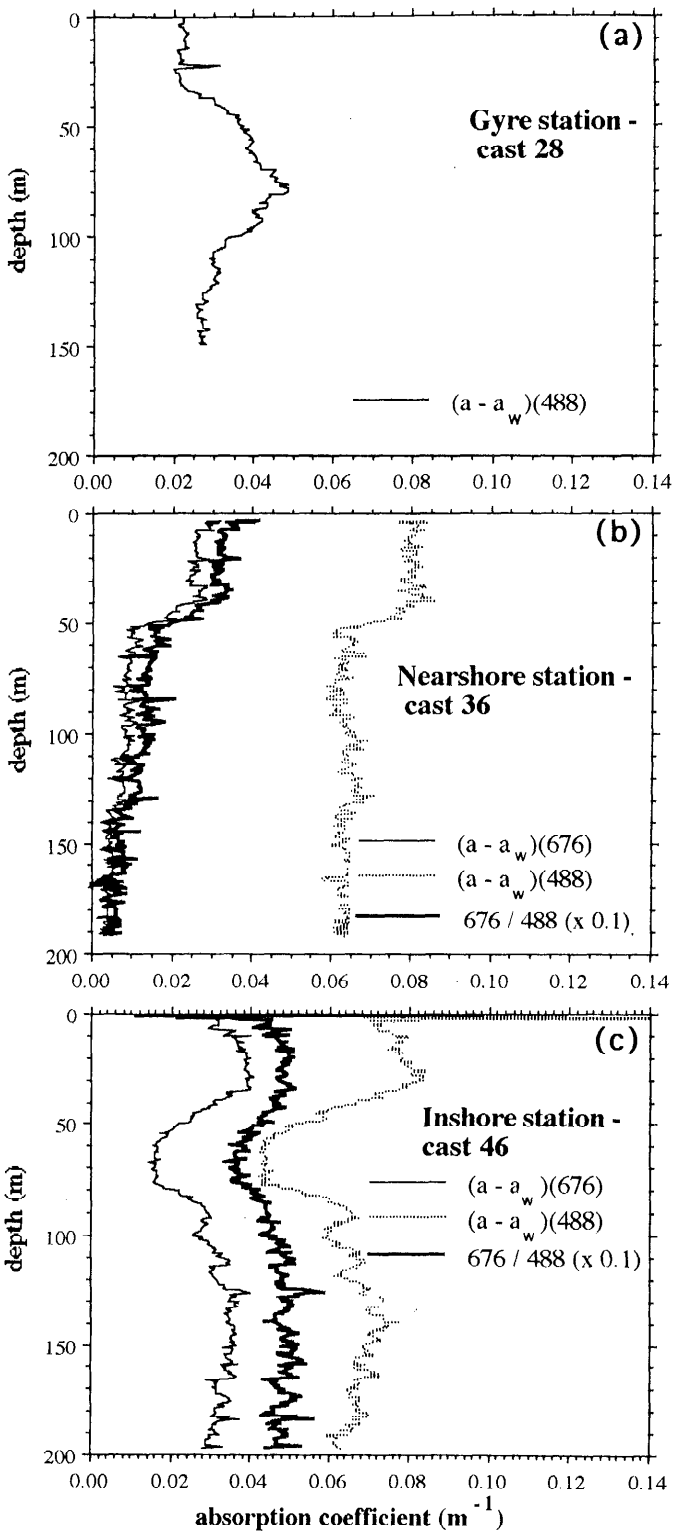

Fig. 8. Typical vertical profiles of the nonwater absorption coefficients $(a - a_w)$ at 676 and 488 nm and of the ratio of these coefficients at the gyre station (no reliable measurements of a at 676 nm were available at this station) and at the nearshore and inshore stations.

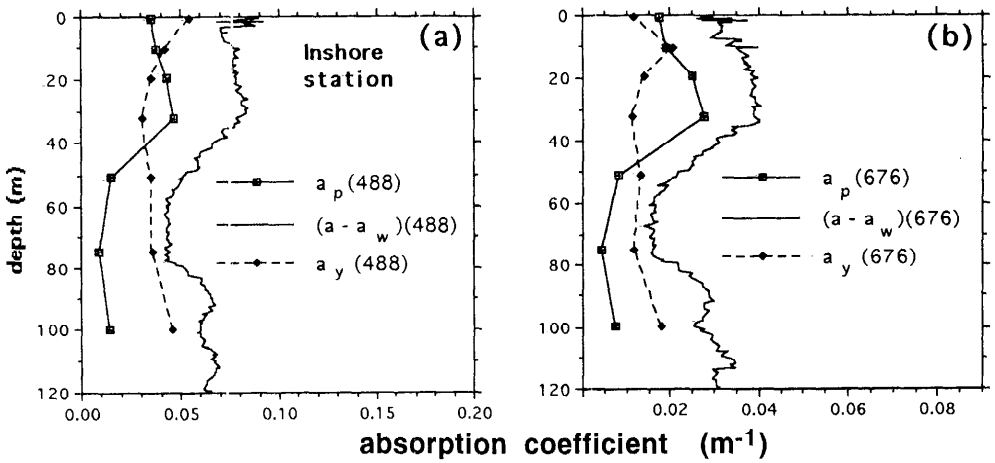

Fig. 9. Vertical profiles at the inshore station of the total (nonwater) absorption coefficients ($a - a_w$) measured in situ and of the particulate absorption coefficients (a_p) measured with the filter technique at 488 and 676 nm. Sampling depths—■. Dashed profiles represent the difference between $a - a_w$ and a_p attributed to dissolved organics.

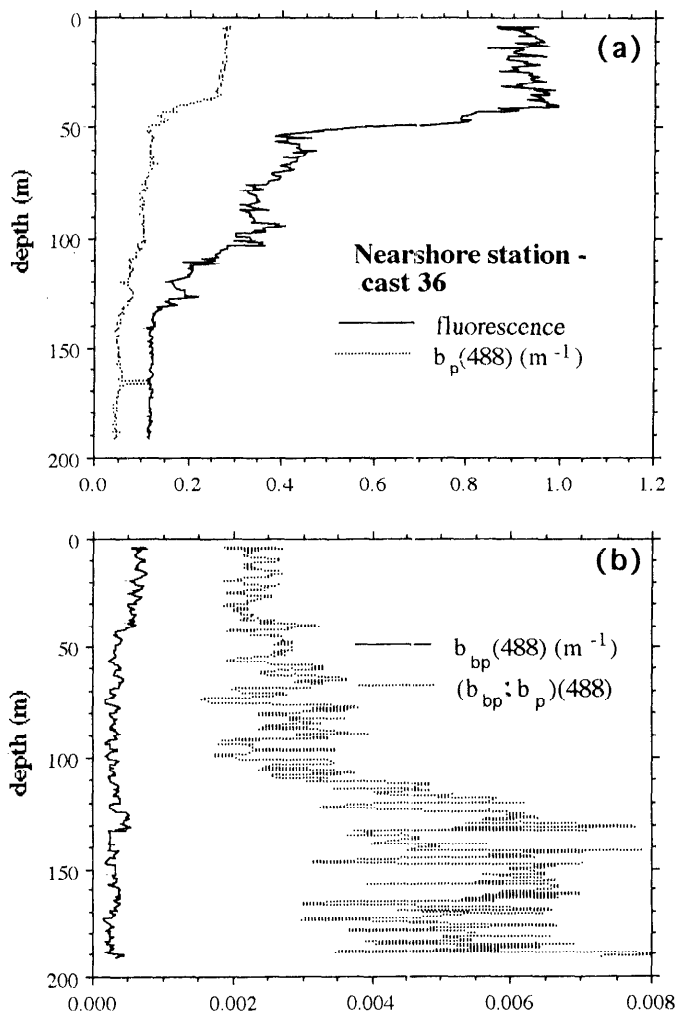

Fig. 10. Typical vertical profiles at the nearshore station of (a) fluorescence (in arbitrary units) and the particulate scattering coefficient (b_p) at 488 nm and (b) the particulate backscattering coefficient (b_{bp}) at 488 nm and the backscattering ratio.

variation may indicate changes in pigment composition and(or) in the amplitude of the package effect and suggests the ability of the absorption meters to detect such changes in the characteristics of phytoplanktonic populations.

Vertical variations of particulate scattering, backscattering, and backscattering ratio—The particulate backscattering coefficient, $b_{bp}(488)$, exhibited a much larger dynamic range at station N than at station I ($<10^{-4}$ m^{-1} to 4×10^{-3} m^{-1} and $<10^{-4}$ to 8×10^{-4} m^{-1}, Fig. 5). The slope of the relationship $b_{bp}(488)$ vs. $(c - c_w)(660)$ was larger by a factor of 5 in the deep waters (80–200 m) of station I than in the surface layer (0–80 m). At station N, there was a similar trend, although it was much less apparent because of the low particle concentration in the deep layer [enhanced values of $b_{bp}(488)$ are observed for $(c - c_w)(660) < 0.15$ m^{-1}]. The average relationships between $b_{bp}(488)$ and $(c - c_w)(660)$ in the surface layers were similar for both stations.

Enhancement of backscattering (relative to seston concentration) from surface to deep waters can also be evidenced in the vertical profiles of the backscattering ratio $(b_{bp} : b_p)(488)$ at station N (Figs. 10b, 11b). This ratio can be computed at each cast where $a(488)$ was measured. $b(488)$ was obtained by subtracting $a(488)$ from $c(488)$, where $c(488)$ was either measured or derived from $c(660)$ (cf. Fig. 2).

At both stations N and I, two dominant modes exist. At station N (Fig. 10b), the backscattering ratio $(b_{bp} : b_p)(488)$ has a value of 2×10^{-3} near the surface and exhibits a 3-fold increase at 120 m, the depth where fluorescence reaches its minimum value (Fig. 10a) and detrital particles presumably become predominant. At station I, $(b_{bp} : b_p)(488)$ displays a still sharper increase (from $\sim 10^{-3}$ to 6×10^{-3}) at 80–100 m before stabilizing at greater depths (Fig. 11b). This increase coincides with the increase in b_p (Fig. 11a) due to resuspension of sediments in the deep layer.

The increase of the backscattering ratio with depth is

likely linked to the increasing proportion of detrital particles compared to living algal cells in the deep layers of both stations. These particles, mainly organic detritus at station N and resuspended sediments at station I, display similar backscattering ratios ($\sim 6 \times 10^{-3}$).

Mie computations performed for spherical and homogeneous particles show that the backscattering ratio increases markedly with the real part of the refractive index of particles, decreases for increasing values of its imaginary part, and varies with the size distribution function (SDF) in a nonmonotonous way (Morel and Bricaud 1986). Phytoplanktonic cells are known to have a low refractive index, typically 1.01–1.07 relative to that of seawater (*see* Aas 1981; Bricaud et al. 1988). They are also characterized by large values of the imaginary indices of refraction, n', at 488 nm ($>10^{-3}$, Ahn et al. 1992), which tend to further decrease their backscattering efficiency. Backscattering ratios of the order of $3–6 \times 10^{-4}$ have been found at 488 nm for some phytoplankters with mean sizes between 4 and 12 μm and may occasionally reach $2–3 \times 10^{-3}$ for very small (<1.5 μm) or very large (>25 μm) species (Ahn et al. 1992).

The refractive index of mineral particles is in the range 1.10–1.25 (*Handbook of chemistry and physics* 1977) and that of particles in various coastal areas falls in the same range (*see* Aas 1981). Few data are available concerning the refractive index of biogenous detrital particles. Considering their organic nature, the index is expected to be intermediate between that of living organisms and that of mineral particles. Also, because very small particles (characterized by a high backscattering efficiency) are predominant in the detrital compartment, these detrital particles are expected to have a backscattering ratio significantly higher than that of living algal cells. The increasing relative concentration of detrital particles from surface to deep waters thus substantiates the increase of $b_{bp}:b_p$ with depth at both stations. Note, however, that backscattering ratios of $\sim 6 \times 10^{-3}$ estimated here for detrital particles are significantly lower than the 2×10^{-2} value introduced by Morel (1988) and Gordon et al. (1988) in their reflectance models. The backscattering ratios estimated for nonchlorophyllous particles (in Case I waters) by Sathyendranath et al. (1989) from spectral reflectance analysis suggest a rather high variability of this parameter (3×10^{-3}–2.5×10^{-2} at 550 nm).

Comparison with the in situ optical coefficients as predicted from Mie theory—Conclusions from the previous qualitative analysis confirm that the in situ optical coefficients are consistent both with associated measurements in the sampled areas and with the range of published values for these coefficients as determined with different approaches. Another important test for the optical instrumentation is the comparison between optical coefficients derived from the in situ instruments and those derived from theory. Mie computations were performed with SDFs measured at sea and plausible values for the refractive indices of the different types of particles as input parameters. A similar approach has already been used by Kitchen and Zaneveld (1990). They compared in situ attenuation coefficients to those provided by a Mie scattering model with a four-component particle population (two refractive indices representing phytoplankton and nonchlorophyllous particles and two size classes with different slopes of the size distribution).

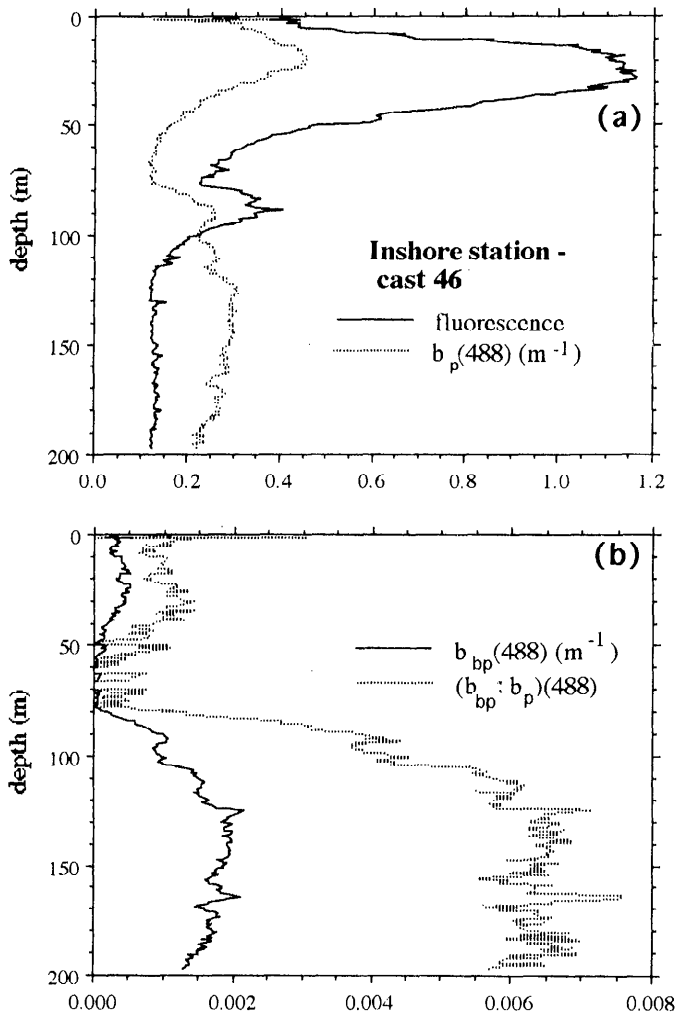

Fig. 11. As Fig. 10, but for the inshore station, day 1.

Most of the size distributions measured during our cruise can be represented by a power law with a unique slope throughout the range 2.4–9 μm, superimposed on an approximately log-normal distribution with a maximum in the range 3.4–3.9 μm (Fig. 12). The maximum in the SDF is very likely due to a monospecific phytoplankton bloom. The power law distribution includes other phytoplankton and nonchlorophyllous (organic or inorganic) particles.

The efficiency factors for scattering (Q_b), backscattering (Qb_b), attenuation (Q_c), and absorption (Q_a) are defined as the ratios of the energy scattered, backscattered, attenuated, and absorbed by a given particle to the energy incident on its cross section. For a given size and assuming a specific (complex) refractive index for each component, they can be computed with the Mie formulas under the proviso that particles are spherical and homogeneous with respect to the refractive index. These assumptions have proven to be admissible for attenuation and total scattering because shape and internal heterogeneities seem to

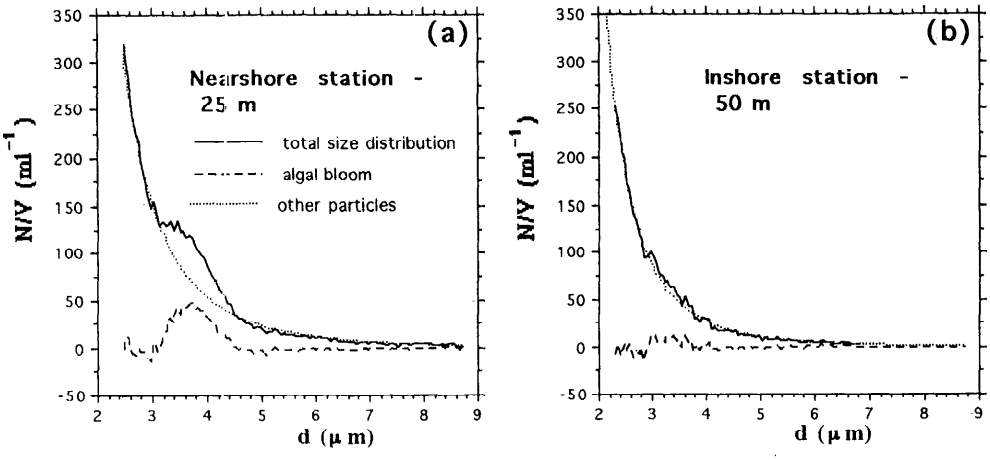

Fig. 12. Particle-size distribution functions as determined at the nearshore station at 25 m and the inshore station at 50 m. These distribution functions have been decomposed into contributions by a monospecific phytoplankton bloom and by other (living and detrital) particles.

have only a limited impact on these coefficients (Bricaud et al. 1988); however, this is not the case for backscattering (*see* Bricaud et al. 1992).

The individual efficiency factors can then be combined according to the SDF to compute the contribution of each component to the bulk particulate coefficients by means of the formula

$$b_i = (\pi/4) \int_0^\infty Q_{b,i}(dN/dD)_i D^2 \, dD \qquad (6)$$

and similar formulas for backscattering, attenuation, and absorption.

As stated previously, the population of particles with the SDF varying as a power law includes both phytoplankton and nonchlorophyllous particles in unknown proportions. One approach, used by Kitchen and Zaneveld (1990), consists of assigning given refractive indices to both categories, assuming that their SDFs have identical slopes in the considered size class, and deriving the relative proportions of particles of each category from the comparison between theoretical and in situ coefficients. As discussed previously, however, the refractive indices of both phytoplankton and nonchlorophyllous particles may be highly variable. Thus we used another approach and attempted to see whether the in situ coefficients could be reproduced by assigning a realistic refractive index to the whole particulate pool (excluding the monospecific bloom). This "bulk" refractive index thus represents an average between those of living algal cells and nonchlorophyllous particles and is expected to increase with the proportion of nonchlorophyllous particles compared to living algal cells. Using such a bulk index for the particulate pool is an approximation similar to that made when assigning a given refractive index to a polyspecific algal population.

For each sample, the observed size distribution $(dN/dD)_{tot}$ (where dN is the particle number density between the diameters D and $D + dD$) was therefore decomposed into two components, $(dN/dD)_{bl}$ and $(dN/dD)_{op}$, corresponding to the phytoplankton bloom and to all other particles. $(dN/dD)_{tot}$ was fitted to a power law (in $N_0 D^{-x}$) over the size class 2.5–3.2 μm, then the SDF of the phytoplankton bloom (when present) was computed over the size range 2.5–8 μm by assuming that the x value was valid over this extended range:

$$(dN/dD)_{bl} = (dN/dD)_{tot} - N_0 D^{-x}. \qquad (7)$$

The SDF measured for the deep samples at station I support the assertion that there is no significant change in the slope when extending the size range to 2.5–8 μm. The values of x obtained for stations N and I at different depths, along with the modal equivalent diameter (D_M) of the SDF of the monospecific bloom and the total particle number (between 2.5 and 8 μm), are shown in Table 2. The x values obtained in the surface waters at station I were unrealistically high (>6, probably due to noise in the first channels of the Coulter Counter) and have been discarded. The x values for other samples were between 3.3 and 4.4, consistent with the commonly observed range for marine particles (Brun-Cottan 1971; Sheldon et al. 1972; Kitchen and Zaneveld 1990).

The measured SDF must be extrapolated from the range 2.5–8 μm toward smaller and larger sizes. For practical computations the above integrals have been limited to the size range 0.3–20 μm. Using Mie theory, Morel and Ahn (1991) demonstrated that for an SDF following a Junge law in $D^{-4.25}$, the particles in the size range 1–10 μm (with an average refractive index of 1.05) contribute ~70% of the total scattering. Therefore, possible variations in the exponent of the Junge law outside the range 2.5–8 μm should have a limited impact on the final b_{op} values. Limiting the integration of $Q_{b,op}$ to the range 0.3–20 μm provides b_{op} with ~5% error (Morel and Ahn 1991, their figure 9b). The situation is quite different for backscattering because the most efficient contributors (accounting for ~85% of the total backscattering for the same

Table 2. Values of the exponents (x) obtained when fitting the SDFs, as measured with a Coulter Counter to power laws ($N_0 D^{-x}$) over the size range 2.5–3.2 μm, modal equivalent diameter (D_M) of the SDF derived for the monospecific phytoplankton bloom when present (*see text and Fig. 12*), total particle number per ml (N/V) between 2.5 and 8 μm, algal cell number corresponding to the bloom ($N/V)_{bl}$, values of the complex refractive index for all other particles ($n_{op} - in'_{op}$) as obtained from the comparison between theoretical and experimental absorption and scattering coefficients, particulate backscattering coefficients (b_{bp}) at 488 nm computed from the refractive index and the SDF of the particulate pool (the contribution of the bloom was negligible each time). The value of the refractive index in parentheses is considered questionable; therefore no corresponding value of $b_{bp}(488)$ is given.

	x	D_M (μm)	(N/V) (ml^{-1})	$(N/V)_{bl}$ (ml^{-1})	$n_{op} - in'_{op}$	$b_{bp}(488)$ (m^{-1})
Nearshore station (N)						
0 m	3.42	3.9	6,600	654	1.050–0.0015i	3.7×10^{-4}
20 m	3.30	3.7	7,328	487	1.016–0.0013i	0.3×10^{-4}
25 m	3.74	3.7	5,544	723	1.030–0.0018i	1.2×10^{-4}
65 m	3.70*	—	1,332	—	1.055–0.0018i	1.8×10^{-4}
100 m	3.58	3.9	6,700	908	(1.010)–0.0003i	—
Inshore station (I)						
50 m	4.17†	—	2,662	—	1.045–0.0015i	3.0×10^{-4}
75 m	4.42†	—	2,394	—	1.040–0.0007i	3.1×10^{-4}
100 m	4.42†	3.4	6,373	928	1.054–0.0005i	7.4×10^{-4}

* Fit over the size range 1.5–2.2 μm (SDF measured with the 30-μm aperture).
† Fit over the size range 2.4–6.8 μm.

exponent and refractive index) are in the range 0.05–0.5 μm. The extrapolation of the Junge law outside the measurement range is therefore much more questionable, and the quality of the b_b coefficients obtained with this method could not be ascertained. We have therefore limited the comparison of the experimental and theoretical coefficients to total scattering.

For a given SDF, the efficiency factor for absorption, Q_a, is determined by the imaginary part of the refractive index of particles. Inversely, at a given station and depth, the particulate absorption coefficient (a_p) measured with the filter technique can be used to evaluate the imaginary part of refractive index for the particulate pool. Despite the comparatively high n' value for algal cells (2×10^{-3}–2×10^{-2} at 488 nm, Ahn et al. 1992), the contribution of the monospecific bloom to absorption is one order of magnitude lower than the contribution of the other particles due to the numerical predominance of these other particles (Fig. 13a). The imaginary part of the bulk refractive index for the other particles (n'_{op}), was adjusted by trial and error to fit the experimental value of a_p. The values of $n'_{op}(488)$ obtained with this method range between 0.0003 and 0.0018 (Table 2). The lowest values are observed in deep waters, consistent with the virtual absence of living algal cells.

For each case, with the n'_{op} value and a typical value of n'_{bl} (chosen equal to 0.01), the relative contributions of both components to total scattering can then be computed (Eq. 6) as functions of the respective real parts of refractive index, n_{op} and n_{bl} (Fig, 13b). As for absorption, the contribution of the monospecific bloom to total scattering seems to be negligible compared to that of other particles, whatever the value of n_{bl} (in the typical range 1.01–1.04). The amplitude of total scattering therefore is entirely determined by the value of $n_{op}(488)$, which can be adjusted to reproduce the observed value of $b_p(488)$ (Table 2).

Nonchlorophyllous particles are expected to be mostly organic at station N and within the 0–100-m layer at station I. The values of n_{op} (1.010–1.055) are in the range expected for a mixture of living algal cells and organic detrital particles. At station N and near the fluorescence maximum (20 and 25 m), n_{op} is relatively low (1.016–1.030), consistent with the expected predominance of living cells. At other depths, the n_{op} values are higher (1.040–1.055), indicating a higher proportion of detrital particles. The exception is the n_{op} value at 100 m for station N (1.010), which very likely is underestimated because at this depth fluorescence is close to its minimum value (*see Fig. 6b*) and detrital particles predominate, as attested by the very low n'_{op} value.

Considering the uncertainties of the measured SDF, of the extrapolation of these SDFs toward very small sizes, and the assumptions made for theoretical computations (sphericity and homogeneity of all particles), it is encouraging that the in situ absorption and scattering values, on the whole, can be reproduced with the measured SDF and a set of plausible values for the complex refractive index of the particulate pool. As stated previously, an accurate comparison between the theoretical and measured backscattering coefficients cannot be performed. However, note that the computed b_{bp} coefficients (indicated in Table 2) are of the same order of magnitude as the measured coefficients and lower by a factor of 2–3, which is easily accounted for by the exclusion of the very small (<0.3 μm) particles in the theoretical computations.

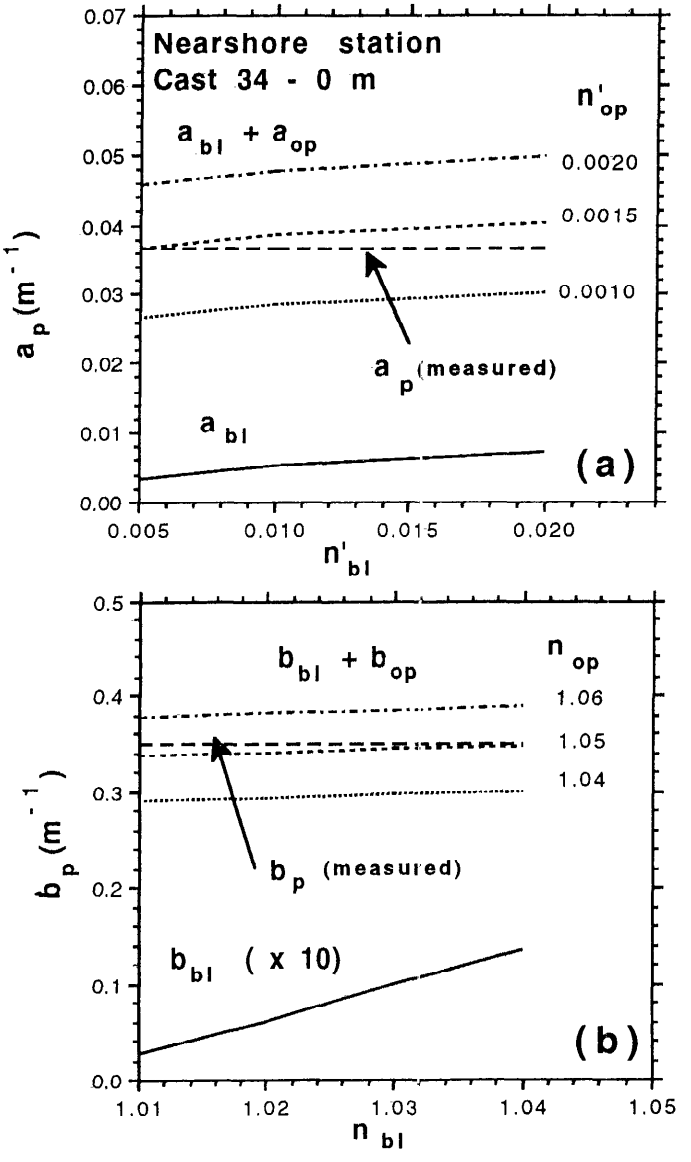

Fig. 13. [a.] Absorption coefficients of phytoplanktonic cells in the monospecific bloom (a_{bl}) and of the total particulate pool ($a_{bl} + a_{op}$) at 488 nm as functions of the imaginary part of the refractive index of phytoplanktonic cells in the bloom (n'_{bl}). Three different values of the imaginary part (n'_{op}) of the bulk refractive index of particles (bloom excluded) are shown. The value of total particulate absorption, a_p, as measured with the filter technique is shown as a horizontal dashed line. [b.] As in panel a for the scattering coefficient at 488 nm and for the real parts of the refractive index of the two components, n_{bl} and n_{op}. The imaginary parts of the refractive index used in the computations are those estimated from panel a. The in situ particulate scattering, $b_p(488)$, shown as a horizontal dashed line was derived by difference from the attenuation and absorption measurements. The example shown is for the nearshore station at 0 m. The values of the absorption and scattering coefficients have been computed with a Mie scattering model (*see text and Table 2*).

Although the refractive indices are in the same range inshore and nearshore, the b_{bp} coefficients, on average, are higher inshore, likely because of the increased importance of the smaller particles as shown by higher x values (Table 2).

Conclusions

The inherent optical properties (Preisendorfer 1976), absorption, attenuation, total scattering, and backscattering coefficients, are independent of the radiative field and, therefore, are more easily interpreted than the apparent optical properties. Advances in technology now make them more accessible to in situ measurement. The development and use of optical instrumentation in view of such measurements has been strongly recommended (e.g. for continuous monitoring of seawater optical properties on moorings) (ABOOS Meeting, Monterey, April 1992).

The principle of the reflective tube for measuring absorption has proven reliable considering these first measurements. As is true for spectrophotometric methods in the laboratory, the scattering contribution to the measured signal must be evaluated to obtain accurate values of in situ absorption. Because scattering in the visible part of the spectrum may be an order of magnitude higher than absorption, an error of 0.01 on the correction factor $k = (a_m - a)/b$ (i.e. an absolute error of 1% on the percentage of scattering detected) leads to an error of ~10% on a. Therefore, using a correction factor based on "typical" volume scattering functions may lead to questionable coefficients. The reflective tube measurements in the infrared region (750 nm) can provide useful guidelines for empirically estimating this correction factor. Because absorption by pure water at this wavelength varies with temperature, it has been recommended that infrared absorption measurements near 710 nm be used (Pegau and Zaneveld 1993).

In view of evaluating the scattering contribution to the measured absorption signal, we also recommend simultaneous measurements with the absorption meter and transmissometer at the same wavelength. In the next generation of spectral sensors, simultaneous measurements of a and c at several wavelengths (including some wavelengths where $a \ll c$) will allow a more accurate estimate of the scattering contribution and its spectral variations. Correcting attenuation coefficients for the scattering contribution is much less critical than for absorption; because $b < c$, an error of 0.01 on the correction factor leads to a <1% error on c.

The red-to-blue absorption ratio, $a(676):a(488)$, can be used to provide information on the spectral behavior of absorption by particles throughout the water column. Absorption measurements suggest that phytoplankton had higher red-to-blue absorption ratios at the inshore station than at the nearshore station, which might indicate differences in pigment composition or in the amplitude of the package effect. Absorption by detrital particles (mostly organic nearshore and mineral inshore) also exhibited different behaviors, with a stronger spectral selectivity

nearshore. Evaluating the variability of the spectral dependence of absorption coefficients provides the first step toward determining the characteristics of organic and inorganic materials in seawater by means of optical measurements.

Simultaneous absorption and attenuation measurements allow calculation of in situ total scattering—a little-documented parameter usually derived from measurements at selected angles. In combination with backscattering measurements, we can obtain profiles of the backscattering ratio. As expected, this ratio was relatively sensitive to, and therefore informative about, vertical changes in particle composition. The prototype backscatterometer is still in a preliminary stage, with limited sensitivity and lack of accurate calibration procedures. These first results, however, are extremely encouraging concerning the feasibility of in situ backscattering measurements.

We compared experimental in situ scattering coefficients to those derived from a Mie scattering model, with the measured particle size distributions and a range of realistic values for the refractive indices of the particulate pool as input parameters and found agreement within this range. This agreement demonstrates that closure models can be successful and efficient in relating the optical properties of individual particles to bulk measurements on natural populations and to in situ optical properties. We could not, however, make such a comparison for in situ backscattering for lack of information concerning the SDF of the submicron particles that primarily govern this coefficient.

References

AAS, E. 1981. The refractive index of phytoplankton. Univ. Oslo, Inst. Rep. Ser. 46. 61 p.

AHN, Y. H., A. BRICAUD, AND A. MOREL. 1992. Light backscattering efficiency and related properties of some phytoplankters. Deep-Sea Res. **39:** 1835–1855.

AMERICAN INST. PHYSICS. 1972. American Institute of Physics handbook. McGraw-Hill.

BARTZ, R., R. W. SPINRAD, AND J. C. KITCHEN. 1988. A low power, high resolution, in situ fluorometer for profiling and moored applications in waters, p. 157–170. *In* Ocean Optics 9, Proc. SPIE **925.**

———, J. R. V. ZANEVELD, AND H. PAK. 1978. A transmissometer for profiling and moored observations in water, p. 102-108. *In* Ocean Optics 5, Proc. SPIE **160.**

BRICAUD, A., A. L. BEDHOMME, AND A. MOREL. 1988. Optical properties of diverse phytoplanktonic species: Experimental results and theoretical interpretation. J. Plankton Res. **10:** 851–873.

———, A. MOREL, AND L. PRIEUR. 1981. Absorption by dissolved organic matter of the sea (yellow substance) in the UV and visible domains. Limnol. Oceanogr. **26:** 43–53.

———, AND D. STRAMSKI. 1990. Spectral absorption coefficients of living phytoplankton and nonalgal biogenous matter: A comparison between the Peru upwelling and the Sargasso Sea. Limnol. Oceanogr. **35:** 562–582.

———, J. R. V. ZANEVELD, AND J. C. KITCHEN. 1992. Backscattering efficiency of coccolithophorids: Use of a three-layered sphere model, p. 27–33. *In* Ocean Optics 11, Proc. SPIE **1750.**

BRUN-COTTAN, J. C. 1971. Etude de la granulométrie des particules. Mesures effectuées avec un Coulter Counter. Cah. Oceanogr. **23:** 193–205.

CARDER, K. L., R. G. STEWARD, G. R. HARVEY, AND P. B. ORTNER. 1989. Marine humic and fulvic acids: Their effects on remote sensing of ocean chlorophyll. Limnol. Oceanogr. **34:** 68–81.

CULLEN, J. J., C. M. YENTSCH, T. L. CUCCI, AND H. L. MACINTYRE. 1988. Autofluorescence and other optical properties as tools in biological oceanography, p. 149–156. *In* Ocean Optics 9, Proc. SPIE **925.**

DOWNING, J. 1983. An optical instrument for monitoring suspended particulates in ocean and laboratory. Proc. Oceans 83. IEEE.

FRY, E. S., AND G. W. KATTAWAR. 1988. Measurement of the absorption coefficient of ocean water using isotropic illumination, p. 142–148. *In* Ocean Optics 9, Proc. SPIE **925.**

———, ———, AND R. M. POPE. 1992. Integrating cavity absorption meter. Appl. Opt. **31:** 2055–2065.

GARDNER, W. D., P. E. BISCAYE, J. R. V. ZANEVELD, AND M. J. RICHARDSON. 1985. Calibration and comparison of the LDGO nephelometer and the OSU transmissometer on the Nova Scotian Rise. Mar. Geol. **66:** 323–344.

GORDON, H. R., AND A. Y. MOREL. 1983. Remote assessment of ocean color for interpretation of satellite visible imagery: A review. Springer.

———, AND OTHERS. 1988. A semianalytic radiance model of ocean color. J. Geophys. Res. **93:** 10,909–10,924.

HANDBOOK OF CHEMISTRY AND PHYSICS. 1977. 58th Ed. CRC.

ITURRIAGA, R., B. G. MITCHELL, AND D. A. KIEFER. 1988. Microphotometric analysis of individual particle absorption spectra. Limnol. Oceanogr. **33:** 128–135.

KIEFER, D. A., AND B. G. MITCHELL. 1983. A simple, steady-state description of phytoplankton growth based on absorption cross section and quantum efficiency. Limnol. Oceanogr. **28:** 770–776.

KIRK, J. T. O. 1975. A theoretical analysis of the contribution of algal cells to the attenuation of light within natural waters. 2. Spherical cells. New Phytol. **75:** 21–36.

———. 1980. Spectral absorption properties of natural waters: Contribution of the soluble and particulate fractions to light absorption in some inland waters of southeastern Australia. Aust. J. Mar. Freshwater Res. **31:** 287–296.

———. 1992. Monte-Carlo modeling of the performance of a reflective tube absorption meter. Appl. Opt. 31, **30:** 6463–6468.

KITCHEN, J. C., AND J. R. V. ZANEVELD. 1990. On the noncorrelation of the vertical structure of light scattering and chlorophyll *a* in Case 1 waters. J. Geophys. Res. **95:** 20,237–20,246.

MITCHELL, B. G. 1990. Algorithms for determining the absorption coefficient of aquatic particulates using the quantitative filter technique (QFT), p. 137–148. *In* Ocean Optics 10, Proc. SPIE **1302.**

———, AND D. A. KIEFER. 1988. Variability in pigment particulate fluorescence and absorption spectra in the northern Pacific Ocean. Deep-Sea Res. **35:** 665–689.

MOORE, C., J. R. V. ZANEVELD, AND J. C. KITCHEN. 1992. Preliminary results from an in situ spectral absorption meter, p. 330–337. *In* Ocean Optics 11, Proc. SPIE, **1750.**

MOREL, A. 1974. Optical properties of pure water and pure sea water, p. 1–24. *In* N. G. Jerlov and E. Steemann Nielsen [eds.], Optical aspects of oceanography. Academic.

———. 1980. In-water and remote measurements of ocean color. Boundary-Layer Meteorol. **18:** 177–201.

———. 1988. Optical modeling of the upper ocean in relation

to its biogenous matter content (Case 1 waters). J. Geophys. Res. **93:** 10,749–10,768.

———. 1991. Light and marine photosynthesis: A spectral model with geochemical and climatological implications. Prog. Oceanogr. **26:** 263–306.

———, AND Y. H. AHN. 1990. Optical efficiency factors of free living marine bacteria: Influence of bacterioplankton upon the optical properties and particulate organic carbon in oceanic waters. J. Mar. Res. **48:** 145–175.

———, AND ———. 1991. Optics of heterotrophic nanoflagellates and ciliates: A tentative assessment of their scattering role in oceanic waters compared to those of bacterial and algal cells. J. Mar. Res. **49:** 177–202.

———, AND A. BRICAUD. 1981. Theoretical results concerning light absorption in a discrete medium, and application to specific absorption of phytoplankton. Deep-Sea Res. **28:** 1375–1393.

———, AND ———. 1986. Inherent optical properties of algal cells including picoplankton: Theoretical and experimental results, p. 521–559. *In* Can. Bull. Fish. Aquat. Sci. 214.

MORROW, J. H., W. S. CHAMBERLIN, AND D. A. KIEFER. 1989. A two-component description of spectral absorption by marine particles. Limnol. Oceanogr. **34:** 1500–1509.

OISHI, T. 1990. Significant relationships between the backward scattering coefficient of sea water and the scatterance at 120°. Appl. Opt. **29:** 4658–4665.

PAK, H., D. A. KIEFER, AND J. C. KITCHEN. 1988. Meridional variations in the concentration of chlorophyll and microparticles in the North Pacific Ocean. Deep-Sea Res. **35:** 1151–1171.

———, J. R. V. ZANEVELD, AND J. C. KITCHEN. 1980. Intermediate nepheloid layers observed off Oregon and Washington. J. Geophys. Res. **85:** 6697–6708.

———, ———, AND R. W. SPINRAD. 1984. Vertical distribution of suspended particulate matter in the Zaire River, estuary and plume. Neth. J. Sea Res. **17:** 412–425.

PEGAU, W. S., AND J. R. V. ZANEVELD. 1993. Temperature-dependent absorption in the red and near-infrared portions of the spectrum. Limnol. Oceanogr. **38:** 188–192.

PETZOLD, T. J. 1972. Volume scattering functions for selected waters. Scripps Inst. Oceanogr. SIO Ref. 72–78.

PREISENDORFER, R. W. 1976. Hydrologic optics, V. 1. NOAA.

ROESLER, C. S., M. J. PERRY, AND K. L. CARDER. 1989. Modeling in situ phytoplankton absorption from total absorption spectra in productive inland marine waters. Limnol. Oceanogr. **34:** 1510–1523.

SATHYENDRANATH, S., L. PRIEUR, AND A. MOREL. 1989. A three-component model of ocean colour and its application to remote sensing of phytoplankton pigments in coastal waters. Int. J. Remote Sensing **10:** 1373–1394.

SHELDON, R. W., A. PRAKASH, AND W. H. SUTCLIFFE, JR. 1972. The size distribution of particles in the ocean. Limnol. Oceanogr. **17:** 327–340.

TAM, A. C., AND C. K. N. PATEL. 1979. Optical absorptions of light and heavy water by laser optoacoustic spectroscopy. Appl. Opt. **18:** 3348–3358.

TRÜPER, H. G., AND C. S. YENTSCH. 1967. Use of glass fiber filters for the rapid preparation of in vivo absorption spectra of photosynthetic bacteria. J. Bacteriol. **94:** 1255–1256.

VOSS, K. J. 1989. Use of the radiance distribution to measure the optical absorption coefficient in the ocean. Limnol. Oceanogr. **34:** 1614–1622.

———. 1992. A spectral model of the beam attenuation coefficient in the ocean and coastal areas. Limnol. Oceanogr, **37:** 501–509.

YENTSCH, C. S. 1962. Measurement of visible light absorption by particulate matter in the ocean. Limnol. Oceanogr. **7:** 207–217.

ZANEVELD, J. R. V., R. BARTZ, AND J. C. KITCHEN. 1990. A reflective-tube absorption meter, p. 124–136. *In* Ocean Optics 10, Proc. SPIE. **1302.**

———, J. C. KITCHEN, A. BRICAUD, AND C. MOORE. 1992. Analysis of in situ spectral absorption meter data, p. 187–200. *In* Ocean Optics 11, Proc. SPIE **1750.**

Submitted: 2 August 1993
Accepted: 1 July 1994
Amended: 13 September 1994